pVT behaviour of hydrophilic and hydrophobic eutectic solvents

Víctor Hernández-Serrano [a], José Muñoz-Embid [a,b], Fernando Bergua [a,b], Carlos Lafuente [a,b], Manuela Artal [a,b,*]

[a] Departamento de Química Física, Facultad de Ciencias, Universidad de Zaragoza, Zaragoza, Spain
[b] Instituto Agroalimentario de Aragón - IA2 (Universidad de Zaragoza - CITA), Zaragoza, Spain

ARTICLE INFO

ABSTRACT

Among the basic principles of green chemistry is the search for less harmful alternative solvents than conventional solvents. Knowing the thermophysical properties of fluids under different pressure and temperature conditions is essential to propose them. Herein, we present data on the densities at several pressures (from 0.1 to 65 MPa) and temperatures (from 283.15 to 338.15 K) of two deep eutectic solvents with hydrophilic characteristics (choline chloride + ethylene glycol or glycerol) and two eutectic solvents with hydrophobic characteristics (camphor + thymol or menthol). We used the Tait equation of state to correlate and calculate derived properties. Moreover, we modelled the mixtures with the PC-SAFT equation of state. The results showed that the hydrophilic solvents were more compact than the hydrophobic ones. The former exhibited an abnormal thermal behaviour of the isobaric thermal expansibility. The deviations in the correlation of densities with the thermodynamic model were between 0.5 and 3%. They were lower for the mixtures with weaker interactions.

1. Introduction

Green chemistry is defined as the "design of chemical products and processes to reduce or eliminate the use and generation of hazardous substances". Its definition and concept were first formulated by Anastas and Warner in the 1990s [1,2], and since then, it has had a great impact on society, transcending from the research laboratory to industry and the people. The purpose of green chemistry is to design new profitable and harmless products and processes for human health and the environment. It is characterized by detailed planning of chemical synthesis, reducing the hazards in the stages of a chemical compound's life cycle in an economic way [3]. For this purpose, the elimination of conventional organic solvents is one of the main objectives. Biomass-derived compounds, ionic liquids, supercritical fluids, and eutectic mixtures have been proposed as alternatives [4,5].

Abbott et al. [6] initially classified eutectic solvents into 4 types depending on the nature of their components: (I) organic salt + metal salt; (II) organic salt + hydrated metal salt; (III) organic salt + hydrogen-bond donor (HBD); and (IV) metal salt + HBD. They are denoted as deep eutectic solvents (DESs) because the strong interactions between the components provoke a deep drop in the melting temperature, and the mixture is a stable liquid in a wide concentration range. From an environmental point of view, type (III) is the most interesting. The use of quaternary amines (choline chloride or similar) as organic salts and metabolites (amino acids, sugars, and alcohols, among others) as HBDs allows their classification as natural deep eutectic solvents, NADESs. In the mixture process, a strong H-bond network between the components is established, and a supramolecular structure can be detected [7–10]. Other consequences of the formed net are the hydrophilic character of the liquid and its extremely high viscosity. This latter is the main drawback of type (III) DESs to implement in the industry. These DESs have been the focus of attention since 2003 [11–17] and are widely applied as solvents or catalysts for organic reactions and extraction processes of polar compounds. Recent papers have collected reviews about the applications of DESs as green solvents in different fields: analytical techniques [18–23], extraction of bioactive compounds from natural sources [24–34], biomass valorization [35–37], and pharmacological and cosmetic industries [38–41].

Since 2015, a new type of eutectic solvent, type (V), has been described [42–44]. They are composed of nonionic substances, and most of the mixtures have a hydrophobic nature with intermolecular interactions weaker than those in DESs. Consequently, the drop in the melting temperature concerning the ideal behaviour is usually small, so the acronym hESs could be more suitable [45]. Compounds with therapeutic properties, such as terpenes, carboxylic acids and other active ingredients, are commonly used to obtain hydrophobic eutectics [46].

They have low viscosity and high affinity to nonpolar compounds, so they can be good candidates for solvents in solid–liquid and liquid-–liquid extractions [47–51].

Our group has previously studied the structure and thermophysical behaviour at atmospheric pressure of choline chloride-based DESs with urea, ethylene glycol, glycerol, glucose, citric acid and resorcinol as well as the effect of water in them [7–10,52–54]. We have also characterized terpene-based hESs with thymol, menthol, and carboxylic acids [55–57]. In this work, we carried out the volumetric study under pressure of two binary DESs containing choline chloride and ethylene glycol or glycerol, and two binary hESs with camphor and thymol or menthol.

Replacing old conventional solvents with new and more sustainable solvents requires knowledge of a wide variety of data, including thermodynamic and transport properties. This is because computer tools that include extensive databases are being developed. Those such as the one proposed by the US EPA (PARIS III) use the concept that solvents with similar thermophysical properties have the same solvent capacity [58]. The properties can be obtained by experimental determination or by prediction and correlation using theoretical models such as equations of state. In the case of density at high pressure of viscous liquids such as DESs using vibrating tube densimeters, reliable measurement requires a correction [59,60]. To carry this out, viscosity values at similar p and T ranges are necessary. This fact limits the measurement possibilities, so experimental data on densities in a wide pressure range are very scarce in the literature. For both DESs studied herein, Leron et al. and Crespo et al. published $p\rho T$ values under similar conditions [61–63]. Conversely, densities at atmospheric pressure have been extensively measured. The paper published in 2023 by Mero et al. [64] includes a review of the articles containing data to date. For our hESs, no density data at several pressures were found. We have only found 3 articles that correspond to densities at atmospheric pressure of the T:C (1:1) mixture [65–67].

Regarding the prediction and correlation, the use of equations of state such as PC-SAFT to represent the behavior of systems is widespread [68–70]. However, they must always be previously validated with experimental data.

This work aims to provide basic information to facilitate the change to new eco-friendly solvents in industrial processes. For that, the densities of two deep and two hydrophobic eutectic solvents at several temperatures (283.15 K–338.15 K) and pressures (0.1–65 MPa) are determined and discussed. The studied DESs were mixtures of choline chloride and ethylene glycol or glycerol in a 1:2 mol ratio. The hESs were composed of camphor and thymol (1:1) or menthol (1:2). The values were correlated with the Tait equation and the PC-SAFT equation of state, PC-SAFT EoS. From the experimental data, several derived properties were calculated in the working p and T ranges. They were the isobaric thermal expansibility, the isothermal compressibility, and the internal pressure.
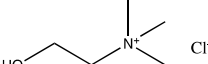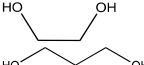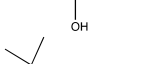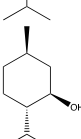
2. Materials and methods

2.1. Materials

The components of the deep eutectic solvents, DESs, were choline chloride, [Ch]Cl, ethylene glycol, EG, and glycerol, G. Due to the hygroscopic character, especially of [Ch]Cl, these substances were dried under vacuum for 24 h before use. The components of the hydrophobic eutectic mixtures, hESs, were camphor, C, thymol, T, and menthol, M, and all were used as supplied. Table 1 reports the characteristics and structures of all chemicals. The four studied samples were choline chloride + ethylene glycol (1:2, mole ratio), choline chloride + glycerol (1:2), camphor + thymol (1:1), and camphor + menthol (1:2). The compositions were chosen so that the mixtures were liquids in a greater temperature range. To prepare them, the components were weighed with a PB210S Sartorius balance ($u(m) = 1 \bullet 10^{-4}$ g), and the liquid phases were obtained by simultaneous stirring and heating. To avoid thermal degradation, a temperature close to 323 K was maintained. The water content was determined by the Karl Fisher method with an automatic titrator Crison KF 1S-2B, and the values were lower than 300 ppm for all mixtures.

2.2. Apparatus

An Anton Paar DMA HP cell was used to measure the density over a wide range of temperatures and pressures. The device was thermostated, and the uncertainty in the temperature was $u(T) = \pm$ 0.01 K. The

Table 1
Relevant properties and structure of pure compounds used in this work.

Chemical (Acronym)	CAS No	Purity([a])	M/g·mol^{-1}	T_m/K	Structure
Choline chloride ([Ch]Cl)	67–48-1	>0.993	139.62	579 ± 7[b]	
Ethylene glycol (EG)	107–21-1	>0.995	62.07	261 ± 2[c]	
Glycerol (G)	56–81-5	>0.999	92.09	290 ± 5[d]	
Camphor (C)	464–49-3	>0.98	152.23	451.5 ± 0.1[c]	
Thymol (T)	89–83-8	>0.985	150.22	322.5 ± 0.5[d]	
Menthol (M)	89–78-1	>0.99	156.27	315.1 ± 0.5[e]	

[a] As stated by the supplier (mass fraction); [b] Ref. [71]; [c] Ref. [72]; [d] Ref. [57]; [e] Ref. [56].

operating pressure was achieved with a handpump 750.1100 (Sitec) and measured with a pressure transducer US181 (Measuring Specialties) with an uncertainty of $u(p) = \pm 0.05$ MPa. The calibration of the high-pressure high-temperature densimeter was performed with four fluids of different densities: dry air, hexane, water and dichloromethane. The combined uncertainty in the measure of density was $U_c(\rho) = \pm 0.1 \; kg \cdot m^{-3}$. Finally, the densimeter was tested with toluene by comparing our data with literature values. The mean relative deviation between both sets of data was $MRD(\rho) = 0.015\%$ [55].

For viscous fluids, the value of the density determined with this type of densimeter must be corrected [59,60]. The apparatus overestimates the density value because the shear forces simulate a higher mass in the tube. The correction, $\Delta\rho$, can be made if fluid density and viscosity data are available under the same temperature and pressure conditions. Herein, the following equation was used:

$$\Delta\rho = \frac{\eta^2}{q_1 + q_2\eta + q_3\eta^2} \tag{1}$$

where ρ and η are the density and viscosity data at each p and T. The $p\eta T$ values were taken from the literature [63]. The q_i fit parameters were $q_1 = 3516.076$, $q_2 = 129.396$, and $q_3 = 843$ [73].

3. Theory

3.1. PC-SAFT EoS

In this work, the volumetric behaviour of the studied mixtures was modelled with the PC-SAFT EoS. The densities and solubility parameters at several pressures and temperatures were calculated and compared with those from the experimental data. This model was developed by Gross and Sadowski [74,75] and is widely used in the literature for all types of fluids. Briefly, the equation of state, EoS, is written in the form of dimensionless Helmholtz energy, $\widetilde{a}$, and is expressed as the sum of an ideal gas, $\widetilde{a}^{id}$, and a residual, $\widetilde{a}^{res}$, contributions. The latter term is calculated with the theory of perturbations. The repulsive interactions are described with the hard-chain reference system, and the attractive ones are considered a disturbance to that. Disregarding polar and ionic contributions:

$$\widetilde{a}^{res} = \widetilde{a}^{hc} + \widetilde{a}^{dis} + \widetilde{a}^{assoc} \tag{2}$$

where $\widetilde{a}^{hc}$, $\widetilde{a}^{dis}$, and $\widetilde{a}^{assoc}$ are the hard-chain, dispersive, and association contributions, respectively. The approach of Chapman [76] and the theory of Barker and Henderson extended to chain molecules [77,78] are used to obtain the first two contributions. Their equations and the one corresponding to the association term are:

$$\widetilde{a}^{hc} = m\widetilde{a}^{hs} - (m-1)\ln g^{hs} \tag{3}$$

$$\widetilde{a}^{dis} = -2\pi\rho m^2 \left(\frac{\varepsilon}{kT}\right)\sigma^3 \sum_{i=0}^{6}\left[a_{0i} + \frac{m-1}{m}a_{1i} + \frac{m-1}{m}\frac{m-2}{m}a_{2i}\right]\eta^i$$
$$- \pi\rho mkT\left(\frac{\partial\rho}{\partial p}\right)_{hc} m^2\left(\frac{\varepsilon}{kT}\right)^2\sigma^3 \sum_{i=0}^{6}\left[b_{0i} + \frac{m-1}{m}b_{1i} + \frac{m-1}{m}\frac{m-2}{m}b_{2i}\right]\eta^i \tag{4}$$

$$\widetilde{a}^{assoc} = \sum_A\left[\ln\left(1 + \rho X^A\Delta\right)^{-1} - \frac{\left(1 + \rho X^A\Delta\right)^{-1}}{2}\right] + \frac{1}{2}S \tag{5}$$

$$\Delta = \kappa^{A_iB_i}\sigma^3 g^{hs}\left[\exp\left(\frac{\varepsilon^{A_iB_i}}{kT}\right) - 1\right] \tag{6}$$

where m is the chain segment number, g^{hs} is the radial pair distribution function of the segments, $\widetilde{a}^{hs}$ is the Helmholtz energy of the hard sphere, ρ is the density, p is the pressure, T is the temperature, σ is the segment diameter, ε is the segment energy, η is the packing fraction, X^A

is the fraction of unbonded monomers, Δ is the tendency to form n-mers, $\kappa^{A_iB_i}$ is the association volume, $\varepsilon^{A_iB_i}$ is the association energy, and S is the number of associated sites of the compound. The parameters $a_{0i}, a_{1i}, a_{2i}, b_{0i}, b_{1i}$, and b_{2i} are called *universal constants* and were obtained from the optimization of the thermodynamic properties of n-alkanes.

To model with this EoS, three geometrical parameters (m, σ and ε) are needed to characterize each pure compound. If the substance can associate, two additional ($\kappa^{A_iB_i}$ and $\varepsilon^{A_iB_i}$) parameters and an association scheme must also be provided. For mixtures, various mixing rules can be applied, and we used the following:

$$\sigma_{ij} = \left(\sigma_i + \sigma_j\right)/2 \tag{7}$$

$$\varepsilon_{ij} = \sqrt{\varepsilon_i\varepsilon_j}\left(1 - k_{ij}\right) \tag{8}$$

$$\kappa^{A_iB_j} = \sqrt{\kappa^{A_iB_i}\kappa^{A_jB_j}} \tag{9}$$

$$\varepsilon^{A_iB_j} = \left(\varepsilon^{A_iB_i} + \varepsilon^{A_jB_j}\right)/2 \tag{10}$$

where the subscripts i and j refer to each of the compounds present in the mixture. The binary interaction parameter, k_{ij}, is calculated by optimizing the thermodynamic properties of the mixture. Then, considering $k_{ij} \neq 0$ implies the loss of the predictive character, turning the model into a correlation. Nevertheless, its inclusion in asymmetric systems is common.

3.2. Tait equation

The Tait equation was used to correlate the experimental density values with the pressure and temperature. The expression is:

$$\rho = \frac{\rho_0(T, p_0)}{1 - C \bullet \ln\left(\frac{B(T)+p}{B(T)+p_0}\right)} \tag{11}$$

where the density at the reference pressure ($p_0 = 0.1$ MPa), ρ_0, and B were fitted to the power expressions:

$$\rho_0(T, p_0) = \sum_{i=0}^{n} A_i \bullet T^i \tag{12}$$

$$B(T) = \sum_{i=0}^{n} B_i \bullet T^i \tag{13}$$

The A_i, B_i, and C are the fitted parameters.

The isobaric thermal expansibility, α_p, the isothermal compressibility, κ_T, and the internal pressure, π_T, were calculated from the density values with the equations:

$$\alpha_p = -\frac{1}{\rho}\left(\frac{\partial\rho}{\partial T}\right)_p \tag{14}$$

$$\kappa_T = \frac{1}{\rho}\left(\frac{\partial\rho}{\partial p}\right)_T \tag{15}$$

$$\pi_T = T\left(\frac{\kappa_T}{\alpha_p}\right)_T - p \tag{16}$$

Both partial derivatives of density were obtained by deriving the equation (11).

4. Results and discussion

In this section, the density, ρ, of four eutectic mixtures at several pressures, p, and temperatures, T, are presented and discussed. For all cases, the pressure ranged from 0.1 to 65 MPa, and the temperature was between 283.15 and 338.15 K. The values are listed in Tables 2 and 3 and represented graphically in Fig. 1. For the DESs, the densities ranged
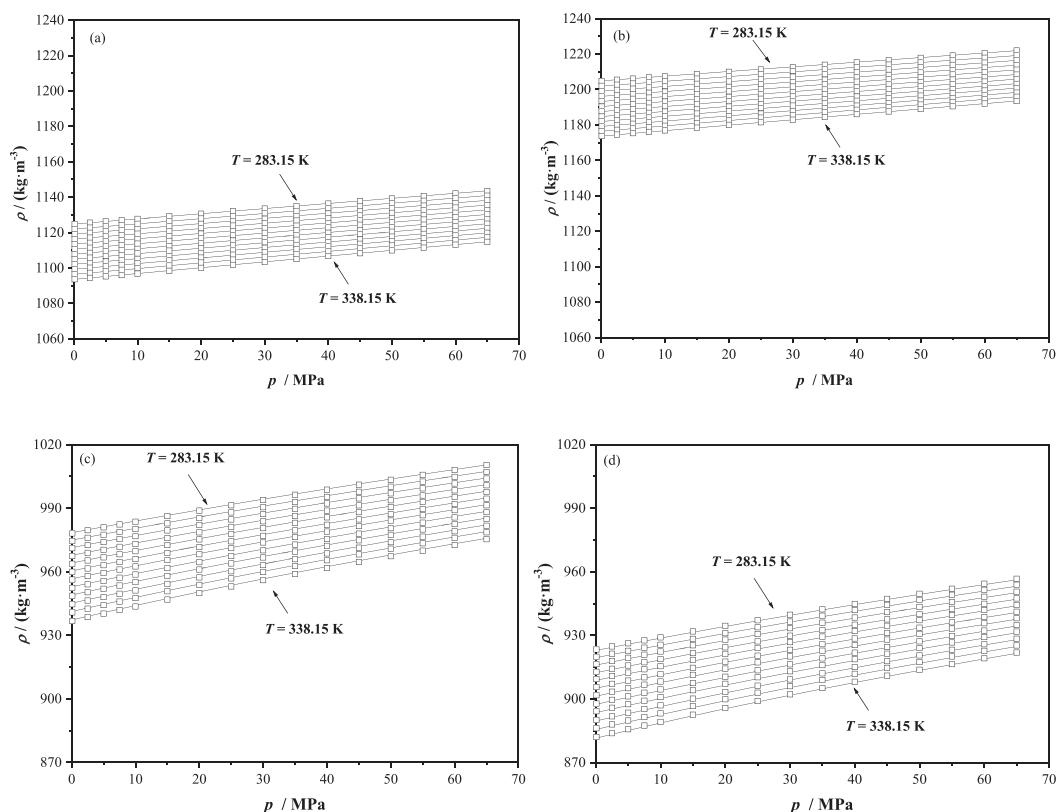
Table 2

Experimental densities, ρ, of the DESs as a function of temperature, T, and pressure, p^a.

T/K	$\rho/(\text{kg} \bullet \text{m}^{-3})$ at p/MPa															
	0.1	2.5	5.0	7.5	10.0	15.0	20.0	25.0	30.0	35.0	40.0	45.0	50.0	55.0	60.0	65.0
Choline chloride:ethylene glycol (1:2)																
283.15	1124.9	1125.6	1126.3	1127.0	1127.7	1129.3	1130.7	1132.1	1133.6	1134.9	1136.4	1137.8	1139.3	1140.7	1142.1	1143.5
288.15	1122.0	1122.8	1123.6	1124.3	1125.0	1126.4	1127.9	1129.4	1130.8	1132.3	1133.7	1135.1	1136.5	1138.0	1139.5	1140.8
293.15	1119.2	1119.9	1120.6	1121.4	1122.0	1123.5	1124.9	1126.4	1127.8	1129.3	1130.8	1132.2	1133.7	1135.2	1136.7	1138.4
298.15	1116.4	1117.1	1117.9	1118.6	1119.4	1120.9	1122.4	1124.0	1125.4	1126.8	1128.3	1129.7	1131.1	1132.6	1134.1	1135.5
303.15	1113.5	1114.2	1115.0	1115.7	1116.4	1117.9	1119.4	1120.9	1122.5	1123.9	1125.4	1126.8	1128.3	1129.7	1131.2	1132.8
308.15	1110.7	1111.5	1112.2	1113.0	1113.8	1115.3	1116.9	1118.4	1119.9	1121.3	1122.9	1124.4	1125.8	1127.3	1128.8	1130.3
313.15	1107.8	1108.6	1109.3	1110.1	1110.8	1112.4	1113.9	1115.5	1116.9	1118.4	1119.9	1121.5	1123.0	1124.5	1126.0	1127.6
318.15	1105.0	1105.8	1106.6	1107.4	1108.2	1109.8	1111.3	1112.9	1114.5	1116.0	1117.5	1119.0	1120.5	1122.1	1123.5	1125.0
323.15	1102.1	1102.8	1103.6	1104.4	1105.1	1106.7	1108.3	1109.9	1111.4	1113.1	1114.6	1116.1	1117.7	1119.3	1120.8	1122.4
328.15	1099.4	1100.2	1101.0	1101.8	1102.6	1104.3	1105.9	1107.5	1109.1	1110.6	1112.2	1113.7	1115.2	1116.8	1118.4	1119.9
333.15	1096.5	1097.3	1098.1	1099.0	1099.8	1101.4	1103.1	1104.7	1106.3	1107.9	1109.4	1111.1	1112.7	1114.2	1115.8	1117.4
338.15	1093.6	1094.4	1095.2	1095.9	1096.8	1098.4	1100.1	1101.8	1103.4	1105.0	1106.8	1108.3	1109.9	1111.5	1113.2	1114.8
Choline chloride:glycerol (1:2)																
283.15	1204.8	1205.5	1206.1	1206.8	1207.4	1208.7	1210.0	1211.3	1212.6	1213.9	1215.3	1216.5	1217.9	1219.2	1220.5	1222.0
288.15	1202.0	1202.7	1203.3	1204.1	1204.8	1206.1	1207.4	1208.7	1210.4	1211.3	1212.6	1214.0	1215.2	1216.5	1217.9	1219.3
293.15	1199.2	1199.8	1200.4	1201.1	1201.8	1203.2	1204.5	1205.9	1207.2	1208.5	1209.9	1211.3	1212.6	1213.9	1215.1	1216.5
298.15	1196.1	1196.8	1197.4	1198.2	1198.8	1200.2	1201.5	1202.8	1204.2	1205.5	1206.9	1208.2	1209.6	1210.9	1212.3	1213.7
303.15	1193.3	1194.0	1194.7	1195.4	1196.1	1197.5	1198.9	1200.3	1201.7	1203.0	1204.4	1205.7	1207.1	1208.5	1209.8	1211.2
308.15	1190.3	1191.0	1191.7	1192.5	1193.2	1194.5	1195.8	1197.2	1198.6	1200.0	1201.4	1202.8	1204.2	1205.6	1207.0	1208.4
313.15	1187.6	1188.3	1189.0	1189.8	1190.4	1191.9	1193.3	1194.8	1196.2	1197.5	1198.9	1200.3	1201.7	1203.0	1204.4	1205.8
318.15	1184.7	1185.4	1186.1	1186.8	1187.5	1188.9	1190.3	1191.8	1193.2	1194.6	1196.0	1197.4	1198.9	1200.3	1201.7	1203.2
323.15	1182.0	1182.7	1183.5	1184.2	1185.0	1186.4	1187.9	1189.4	1190.9	1192.3	1193.6	1195.0	1196.5	1197.9	1199.4	1200.8
328.15	1179.1	1179.9	1180.6	1181.4	1182.1	1183.5	1185.0	1186.4	1187.9	1189.4	1190.9	1192.4	1193.7	1195.2	1196.7	1198.2
333.15	1176.5	1177.2	1178.0	1178.8	1179.5	1181.1	1182.5	1184.1	1185.6	1187.1	1188.6	1190.0	1191.5	1193.0	1194.4	1195.9
338.15	1173.7	1174.5	1175.3	1176.1	1176.9	1178.5	1180.0	1181.5	1182.9	1184.5	1186.0	1187.6	1189.0	1190.5	1192.0	1193.4

^{a} Standard uncertainties are $u(T) = 0.01$ K, $u(p) = 0.05$ MPa and the combined expanded uncertainties are $U_c(\rho) = 0.1$ kg·m^{-3} with 0.95 level of confidence ($k \approx 2$).

Table 3

Experimental densities, ρ, of the hESs as a function of temperature, T, and pressure, p^a.

T/K	ρ/(kg $\bullet$ m^{-3}) at p/MPa															
	0.1	2.5	5.0	7.5	10.0	15.0	20.0	25.0	30.0	35.0	40.0	45.0	50.0	55.0	60.0	65.0
Camphor:thymol (1:1)																
283.15	978.1	979.6	981.0	982.3	983.6	986.3	988.9	991.4	993.8	996.3	998.7	1001.1	1003.4	1005.8	1008.1	1010.4
288.15	974.6	976.0	977.5	978.8	980.2	982.8	985.3	988.0	990.4	992.9	995.4	997.8	1000.2	1002.6	1004.8	1007.1
293.15	971.1	972.6	974.0	975.4	976.8	979.5	982.1	984.7	987.2	989.7	992.2	994.6	997.0	999.4	1001.7	1004.0
298.15	967.4	968.9	970.4	971.8	973.1	975.9	978.6	981.2	983.8	986.3	988.9	991.3	993.7	996.0	998.4	1000.8
303.15	963.8	965.3	966.8	968.3	969.7	972.6	975.3	977.9	980.6	983.1	985.7	988.1	990.6	993.0	995.4	997.7
308.15	960.0	961.5	963.1	964.6	966.0	968.9	971.7	974.3	977.0	979.5	982.2	984.7	987.2	989.6	992.0	994.5
313.15	956.3	958.0	959.5	961.0	962.5	965.5	968.3	971.1	973.8	976.4	979.0	981.5	984.2	986.7	989.1	991.4
318.15	952.4	954.1	955.7	957.2	958.7	961.7	964.5	967.4	970.1	972.8	975.4	978.0	980.6	983.2	985.7	988.1
323.15	948.7	950.3	952.0	953.5	955.1	958.0	961.0	963.9	966.7	969.5	972.2	974.8	977.4	979.9	982.5	984.9
328.15	944.6	946.4	948.1	949.6	951.2	954.3	957.3	960.2	963.1	965.9	968.7	971.4	974.0	976.6	979.1	981.7
333.15	940.8	942.6	944.3	945.9	947.5	950.8	953.8	956.9	959.8	962.7	965.4	968.2	970.9	973.4	976.0	978.6
338.15	936.8	938.6	940.3	942.0	943.6	946.9	950.0	953.0	956.0	959.0	961.8	964.6	967.3	970.0	972.6	975.3
Camphor:menthol (1:2)																
283.15	923.3	924.7	926.2	927.6	929.0	931.8	934.5	937.1	939.7	942.2	944.8	947.2	949.6	952.0	954.4	956.7
288.15	919.9	921.3	922.7	924.2	925.5	928.4	931.0	933.8	936.5	939.3	941.9	944.4	946.8	949.2	951.5	953.9
293.15	916.4	917.9	919.4	920.9	922.4	925.3	928.0	930.7	933.4	936.0	938.4	940.9	943.4	945.8	948.2	950.6
298.15	912.8	914.2	915.8	917.3	918.8	921.6	924.4	927.2	929.9	932.4	935.0	937.5	940.0	942.5	944.9	947.4
303.15	909.4	910.9	912.4	914.0	915.4	918.4	921.3	924.1	926.8	929.4	932.1	934.5	937.1	939.6	942.0	944.4
308.15	905.6	907.1	908.7	910.2	911.7	914.7	917.6	920.4	923.2	925.8	928.5	931.1	933.6	936.1	938.6	941.2
313.15	901.8	903.4	905.1	906.7	908.2	911.4	914.3	917.2	920.1	922.8	925.4	928.0	930.7	933.2	935.7	938.1
318.15	897.8	899.6	901.2	902.9	904.5	907.5	910.5	913.5	916.3	919.1	921.8	924.5	927.2	929.7	932.2	934.8
323.15	894.2	895.9	897.5	899.2	900.9	904.1	907.2	910.2	913.0	915.9	918.7	921.4	924.0	926.6	929.2	931.8
328.15	890.2	891.8	893.5	895.3	897.0	900.2	903.3	906.3	909.2	912.1	915.0	917.8	920.6	923.2	925.8	928.4
333.15	886.2	888.0	889.8	891.5	893.2	896.7	899.8	903.0	906.0	909.0	911.9	914.7	917.4	920.0	922.7	925.2
338.15	882.1	883.8	885.7	887.5	889.2	892.6	895.8	899.0	902.2	905.1	908.1	911.0	913.8	916.4	919.2	921.9

[a] Standard uncertainties are $u(T) = 0.01$ K, $u(p) = 0.05$ MPa and the combined expanded uncertainties are $U_c(\rho) = 0.1$ kg·m^{-3} with 0.95 level of confidence ($k \approx 2$).

Fig. 1. Density, ρ, of the studied mixtures as a function of temperature, T, and pressure, p. (a) [Ch]Cl:EG (1:2); (b) [Ch]Cl:G (1:2); (c) C:T (1:1); (d) C:M (1:2). (□) experimental data, (—) Values calculated with the Tait equation.

Table 4

Pure compound PC-SAFT parameters used for modelling the eutectic mixtures. The 2B autoassociation scheme was considered.

Compound	m	σ/ Å	ε/ K	$\kappa^{A_iB_i}$	$\varepsilon^{A_iB_i}$/K	Ref.
Choline chloride ([Ch]Cl)	13.02	2.368	228.07	0.2	8000	[80]
Ethylene glycol (EG)	2.4366	3.2330	344.06	0.02216	2706.2	[81]
Glycerol (G)	2.0070	3.815	430.82	0.0019	4633.5	[82]
Camphor (C)	3.583	3.984	283.5	0.010	2662.3	This work
Thymol (T)	4.012	3.816	290.22	0.0616	1660.0	[79]
Menthol (M)	4.152	3.903	262.40	0.0996	1785.6	[79]

between 1093.64 and 1223.52 kg • m^{-3}, and the mixture with glycerol was the densest. These values were approximately 20% higher than those for both hESs. A higher value of density may be due to the presence of strong interactions between components or to lower steric hindrance. According to this, the results showed the expected trends. In both DESs, the interactions are mainly electrostatic and hydrogen bonding, and they are hydrophobics in our hESs. Moreover, RMN studies have shown that the supramolecular structure in [Ch]Cl:G is stronger than that in [Ch]Cl:EG due to its increased ability to act as a donor of hydrogen bonds [7]. For both hESs, the interactions are dispersive, but the mixture with thymol was more compact because of the flat structure of the aromatic ring.

In the literature, we have found $p\rho T$ values for the two hydrophilic mixtures with choline chloride, and our data agreed with those [61–63]. For the mixture with EG, the mean relative deviation was lower than 0.11%, with a maximum absolute deviation of 1.7 kg • m^{-3}. For that with G, these values were 0.17% and 2.8 kg • m^{-3}. The graphical comparison is shown in Figure S1. For hESs, only literature values of density at 298.15 K and atmospheric pressure for the C:T (1:1) mixture were found [65–67], and the one published by Abdallah et al. [65] matched with our results.

The validation of the thermodynamic models allows to predict the

Table 5

Mean relative deviations [a,b] in the modelling with the PC-SAFT EoS.

Mixture	k_{ij}	$MRD(p)$
[Ch]Cl:EG (1:2)	0	1.53
	0.082	0.49
[Ch]Cl:G (1:2)	0	2.96
	0.19	0.70
C:T (1:1)	0	0.53
C:M (1:2)	0	0.99

$$MRD(Y) = \frac{100}{n}\sum_{i=1}^{n}\left|\frac{Y_{i,cal} - Y_{i,exp}}{Y_{i,exp}}\right|$$

[b] T_{range} = 283.15–338.15 K; p_{range} = 0.1–65 MPa

behaviour of fluids under different conditions. Here, we have modeled the volumetric behaviour, at several p and T, of DESs and hESs studied with the PC-SAFT EoS. Table 4 collects the five parameters needed for each pure compound. The values were taken from the literature [79] except for camphor, for which they have been obtained in this work. All mixtures were modelled in the predicted version, that is, with a null binary interaction parameter. For DESs, the density was also calculated with $k_{ij} \neq 0$. The deviations between the experimental and calculated data are listed in Table 5 and pictured in Fig. S2. The model well predicted the density for all systems, particularly in those with weaker interactions. The maximum deviation, $MRD(p) = 3.9\%$, was found for [Ch]Cl:G (1:2), and the value decreased to 1.6% when a non-null binary interaction parameter was included.

The values of the density at several pressures and temperatures were correlated with the equation of Tait (eq. (11)–(13)). The values of the coefficients and the relative root-mean-square deviations, $RMSDr(\%)$, between experimental and correlated data are collected in Table 6.

From $p\rho T$ data, several derived properties necessary to design optimal industrial processes can be obtained. The isobaric thermal expansibility, α_p, and the isothermal compressibility, κ_T, allow us to quantify the influence of T and p on ρ. The values obtained with the equations (14) and (15) are reported in Tables S1 to S4 and displayed in Figs. 2 and 3.

Systems with weaker intermolecular interactions have higher values of these properties, as well as a greater effect of pressure and temperature on them. In this work, the full sequences for α_p and κ_T were in agreement with the inverse of the strength of the intermolecular interactions: ([Ch]Cl:G) <([Ch]Cl:EG) ≪(C:T) <(C:M).

For DESs, the α_p values were approximately 2/3 times those for hESs, and the [Ch]Cl:EG mixture had higher thermal expansibility than [Ch]Cl:G. As usual, the expansion capacity decreased with increasing pressure, with a greater slope at higher temperatures. Nevertheless, anomalous thermal behaviour was observed. For the eutectic with EG, α_p decreased to increase the temperature from approximately 12 MPa, and this trend was observed at any pressure for the eutectic with G. This fact, $(\partial\alpha_p/\partial T)\langle 0$, has already been published for other fluids such as ionic liquids and has been related to the presence of ionic interactions [83]. In this paper, the authors concluded that the more condensed a fluid is, the lower the pressure above which abnormal behaviour appears. For hESs, the values were higher for the mixture with menthol, and the expected trends with $(\partial\alpha_p/\partial p)\langle 0$ and $(\partial\alpha_p/\partial T)\rangle 0$ were obtained.

Regarding the isothermal compressibility, κ_T, the values for DESs were up to 3.2 times lower than those for hESs as a consequence of the worse packaging of the latter. This property increased with increasing T and decreasing p. For the hydrophilic mixtures, the difference in the compressibility at maximum and minimum temperatures was similar and slightly decreased with increasing pressure. Therefore, for both DESs, $\Delta\kappa_T(T_{max}, T_{min}) = 44$ and 40 TPa^{-1} at 0.1 and 65 MPa, respectively. The effect of T on κ_T was more marked for hESs: $\Delta\kappa_T(T_{max}, T_{min}) = 174$ and 90 TPa^{-1} for C:T and 198 and 97 TPa^{-1} for C:M. The effect of p

Table 6

Parameters of the Tait equation and relative root mean square deviations, $RMSDr$ [a]

	[Ch]Cl:EG (1:2)	[Ch]Cl:G (1:2)	C:T (1:1)	C:M (1:2)
A_0/(kg • m^{-3})	1280.48	1405.89	1097.57	1013.53
A_1/(kg • m^{-3} • K^{-1})	−0.5341	−0.8294	−0.1460	0.0426
A_2/(kg • m^{-3} • K^{-2})	−0.000055	0.000422	−0.00097	−0.00128
C	0.2511	0.2434	0.0960	0.0979
B_0/(MPa)	281.36	1097.64	220.02	175.39
B_1/(MPa • K^{-1})	6.4937	2.8105	0.2375	0.3934
B_2/(MPa • K^{-2})	−0.014460	−0.009880	−0.00151	−0.00168
$RMSDr$/%	0.030	0.010	0.044	0.049

[a] $RMSDr/\% = 100\left(\frac{1}{n}\sum_{i=1}^{n}\left(\frac{\rho_{i,corr} - \rho_{i,exp}}{\rho_{i,exp}}\right)^2\right)^{1/2}$; n is the number of points
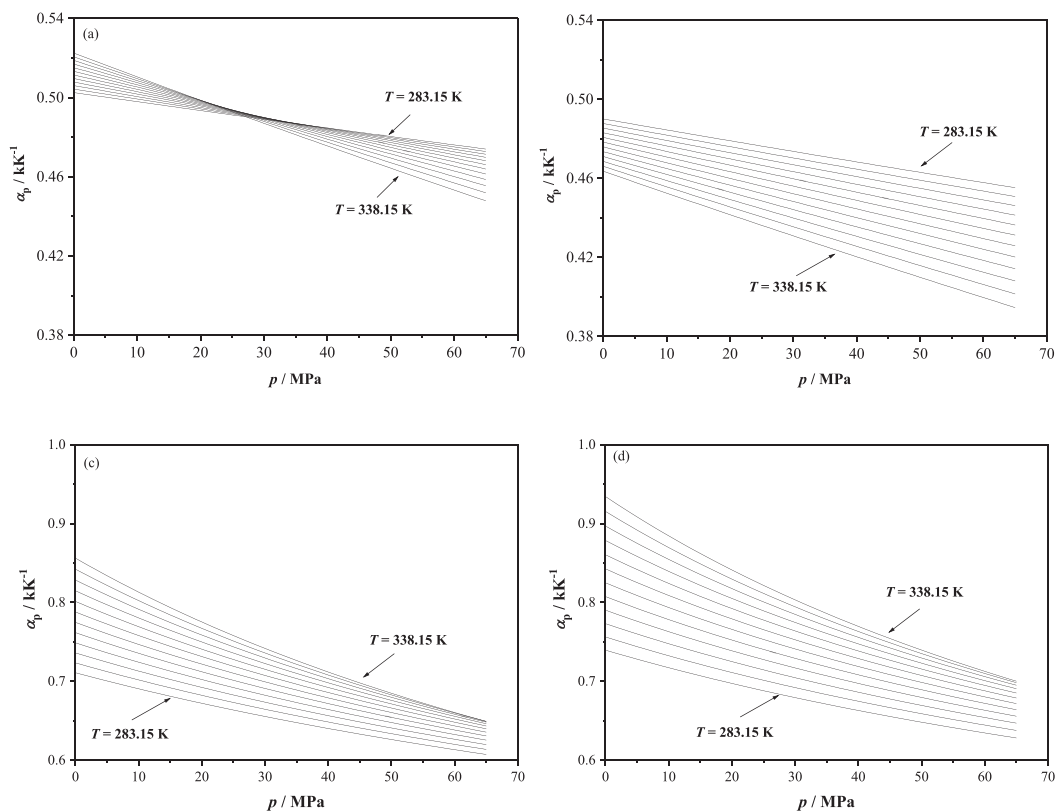
Fig. 2. Isobaric expansibility, α_p, of the studied mixtures as a function of temperature, T, and pressure, p. (a) [Ch]Cl:EG (1:2); (b) [Ch]Cl:G (1:2); (c) C:T (1:1); (d) C:M (1:2).
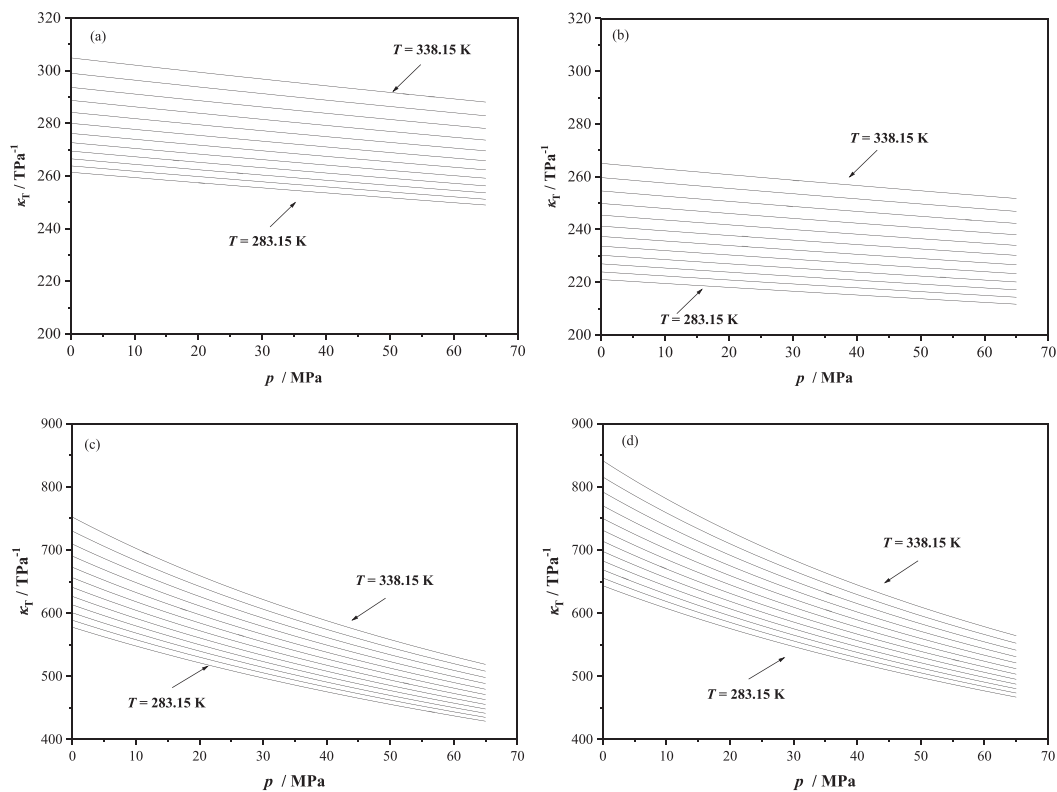

Fig. 3. Isothermal compressibility, κ_T, of DESs as a function of temperature, T, and pressure, p. (a) [Ch]Cl:EG (1:2); (b) [Ch]Cl:G (1:2); (c) C:T (1:1); (d) C:M (1:2).

on κ_T can be quantified in the same way. Then, the calculated values of the differences at 283.15 and 338.15 K were $\Delta\kappa_T(p_{max}, p_{min}) = -12.4$ and -16.8 TPa^{-1} for [Ch]Cl:EG, -9.35 and -13.3 TPa^{-1} for [Ch]Cl:G, -146 and -233 TPa^{-1} for C:T, and -176 and -276 TPa^{-1} for C:M. The relationship of κ_T with p was different for the two types of systems. Direct linearity ($\kappa_T - p$) was found for DESs, and the inverse $\left(\frac{1}{\kappa_T} - p\right)$ was found for hESs. The latter was in agreement with the expression of Wilhelm [84], and the obtained slope ($m = 9$) was close to those for other hydrophobic compounds.

Leron et al. [61,62] published α_p and κ_T values for both DESs. Our α_p data were lower than those under all conditions as can be seen in Figures S3 and S4. The maximum absolute deviations for the mixtures with [Ch]Cl:EG and [Ch]Cl:G were 0.02 and 0.03 kK^{-1}, respectively. Smaller κ_T deviations were obtained for the intermediate p and T values for both mixtures. The maximum difference with our data was 18 TPa^{-1} for the mixture with EG and 22 TPa^{-1} for those containing G.

The internal pressure, π_T, is defined as the change in internal energy of a system when the volume changes in a small isothermal expansion. Then, it is related to the type of prevailing intermolecular forces. More positive π_T values mean stronger attractive forces. Fig. 4 shows the values of π_T at several T and p calculated with the equation (16). According to the meaning of π_T, the ordering values was as expected: $\pi_T([Ch]Cl:G) > \pi_T([Ch]Cl:EG) \gg \pi_T(C:T) > \pi_T(C:M)$. In all mixtures, π_T decreased as p increased. The internal pressure of the [Ch]Cl:G mixture decreased continuously with increasing T, and the rest exhibited a maximum that shifted to lower temperatures at higher pressures. This sign change in the temperature coefficient ($\partial\pi_T/\partial T$) is caused by a change in the structural organization of the liquid and occurs at lower temperatures in systems with weaker interactions [85]. Fluids in which

hydrogen bonding interactions prevail over van der Waals interactions present monotonic behaviour since a small expansion is only capable of significantly modifying weak interactions.

The internal pressure allows to estimate the solubility parameter, δ, in fluids in which the interactions are of physical nature (polar and dispersive) [86]. Therefore, π_T is the square of the volume-dependent cohesion parameter, δ_V. For fluids with interactions of chemical nature such as hydrogen bonding, the cohesive energy density, *CDE*, is increased, appearing as a residual term in the solubility parameter, δ_R. In the two-dimensional plane [87]:

$$CED = \delta^2 = \delta_V^2 + \delta_R^2 = \pi_T + \delta_R^2 \tag{17}$$

Then, the difference between the estimated cohesive energy and the internal pressure could be a measure of the magnitude of the network of hydrogen bonds existing in the fluid. Taking into account that the PC-SAFT EoS has well represented the thermodynamic behaviour of these systems, this model can be used to estimate *CED* and, after, calculate the residual contribution as the mentioned difference. The δ_R^2 was much higher for the hydrophilic mixtures, which is in agreement with their stronger H-bond network. The highest values were obtained at the conditions for which the H-bond formation was favored, that is, at the highest pressure and the lowest temperature. The maxima values of δ_R^2 were 12 and 290 MPa for hESs and DESs, respectively.

5. Conclusions

The volumetric behaviour of two hydrophilic, DESs, and two hydrophobic, hESs, eutectic solvents are presented at several pressures and temperatures. The studied systems were choline chloride + ethylene
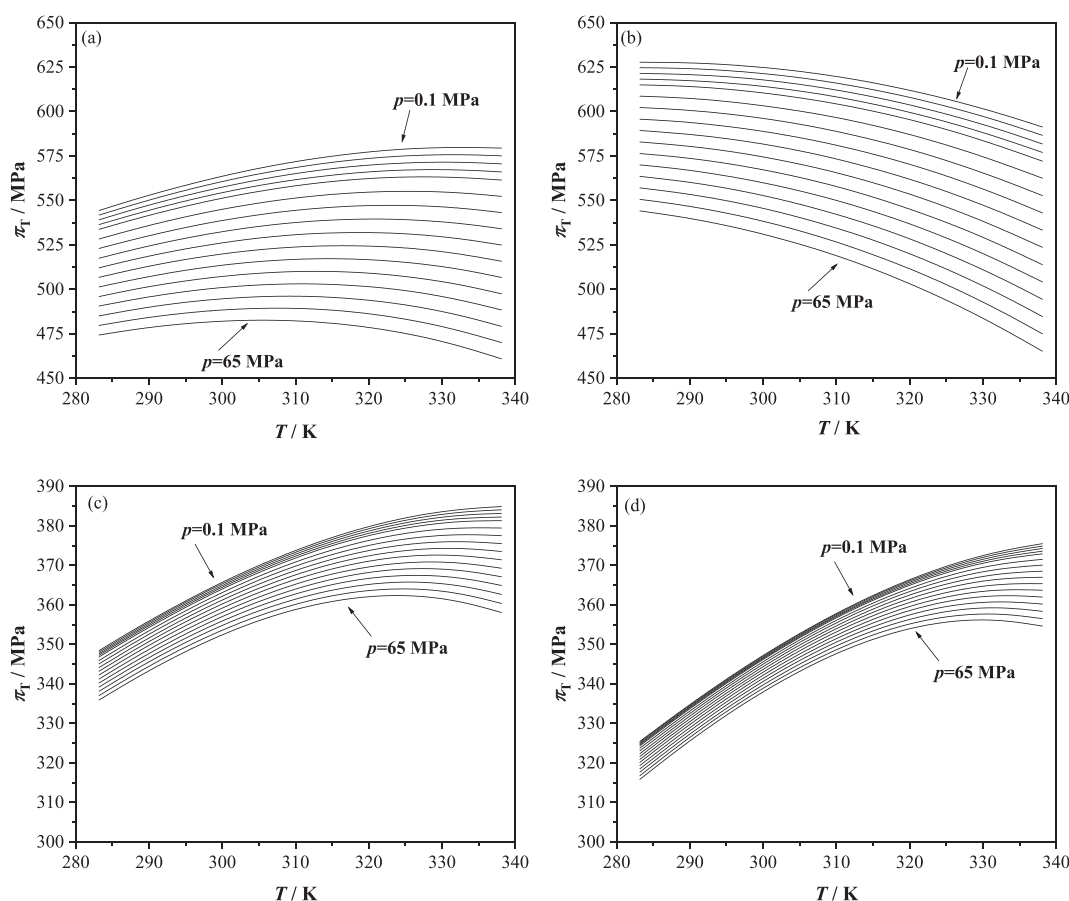

Fig. 4. Internal pressure, π_T, of the studied mixtures as a function of temperature, T, and pressure, p. (a) [Ch]Cl:EG (1:2); (b) [Ch]Cl:G (1:2); (c) C:T (1:1); (d) C:M (1:2).

glycol or glycerol and camphor + thymol or menthol. The measured densities were correlated with the Tait equation and modelled with the PC-SAFT equation of state. From the experimental results, the isobaric thermal expansibility, the isothermal compressibility, and the internal pressure were calculated. Two ranges of values were obtained for the two types of mixtures. The DESs were denser and more compact mixtures than the hESs, in agreement with the stronger hydrogen bond network. The sequence was ([Ch]Cl:G) >([Ch]Cl:EG) ≫ (C:T) >(C:M). The PC-SAFT equation of state was validated for these mixtures in the *p* and *T* ranges of the study. The deviations with the predictive model were less than 3% and 1% for DESs and hESs, respectively. Unlike hESs, a negative temperature coefficient of α_p was found for both DESs. Therefore, we can conclude that hydrophilic mixtures are more condensed fluids than hydrophobic mixtures. Except for ([Ch]Cl:G), a sign change in the temperature coefficient of π_T was observed, indicating a change in the structure of the liquid to change *T*. Finally, a comparison between π_T and the cohesive energy density estimated with the EoS showed, as expected, the great difference between the two concepts for systems containing H-bonds.

CRediT authorship contribution statement

Víctor Hernández-Serrano: Investigation, Formal analysis. **José Muñoz-Embid:** Investigation, Methodology. **Fernando Bergua:** Formal analysis. **Carlos Lafuente:** Validation, Writing – original draft, Funding acquisition. **Manuela Artal:** Writing – original draft, Writing – review & editing.

Declaration of Competing Interest

The authors declare that they have no known competing financial interests or personal relationships that could have appeared to influence the work reported in this paper.

Data availability

Data are in the Supplementary File

Acknowledgments

Appendix A. Supplementary material

Supplementary data to this article can be found online at https://doi.org/10.1016/j.molliq.2023.122019.

References

[1] P. Anastas, J.C. Warner, Green Chemistry: theory and practice, Oxford University Press, Oxford, 2000.

[2] T.S. Anastas, P.T., Williamson, Green Chemistry. Designing Chemistry for the Environment., America Chemical Sociaty, Washington, 1996.

[3] P. Anastas, N. Eghbali, Green Chemistry: Principles and Practice, Chem. Soc. Rev. 39 (2010) 301–312, https://doi.org/10.1039/B918763B.

[4] S. Kar, H. Sanderson, K. Roy, E. Benfenati, J. Leszczynski, Green Chemistry in the Synthesis of Pharmaceuticals, Chem. Rev. 122 (2022) 3637–3710, https://doi.org/10.1021/acs.chemrev.1c00631.

[5] X. Meng, Y. Wang, A.J. Conte, S. Zhang, J. Ryu, J.J. Wie, Y. Pu, B.H. Davison, C. G. Yoo, A.J. Ragauskas, Applications of biomass-derived solvents in biomass pretreatment – Strategies, challenges, and prospects, Bioresour. Technol. 368 (2023), 128280, https://doi.org/10.1016/j.biortech.2022.128280.

[6] A.P. Abbott, J.C. Barron, K.S. Ryder, D. Wilson, Eutectic-Based Ionic Liquids with Metal-Containing Anions and Cations, Chem. A Eur. J. 13 (2007) 6495–6501, https://doi.org/10.1002/chem.200601738.

[7] I. Delso, C. Lafuente, J. Muñoz-Embid, M. Artal, NMR study of choline chloride-based deep eutectic solvents, J. Mol. Liq. 290 (2019), 111236, https://doi.org/10.1016/j.molliq.2019.111236.

[8] L. Lomba, F. Tucciarone, B. Ginera, M. Artal, C. Lafuente, Thermophysical characterization of choline chloride: Resorcinol and its mixtures with water, Fluid Phase Equilib. 557 (2022), 113435, https://doi.org/10.1016/j.fluid.2022.113435.

[9] F. Bergua, I. Delso, J. Muñoz-Embid, C. Lafuente, M. Artal, Structure and properties of two glucose-based deep eutectic systems, Food Chem. 336 (2021), 127717, https://doi.org/10.1016/j.foodchem.2020.127717.

[10] N. López, I. Delso, D. Matute, C. Lafuente, M. Artal, Characterization of xylitol or citric acid:choline chloride:water mixtures: Structure, thermophysical properties, and quercetin solubility, Food Chem. 306 (2019), 125610, https://doi.org/10.1016/j.foodchem.2019.125610.

[11] A.P. Abbott, G. Capper, D.L. Davies, R.K. Rasheed, V. Tambyrajah, Novel solvent properties of choline chloride/urea mixtures, Chem. Commun. 9 (2003) 70–71, https://doi.org/10.1039/b210714g.

[12] A. Paiva, R. Craveiro, I. Aroso, M. Martins, R.L. Reis, A.R.C. Duarte, Natural Deep Eutectic Solvents – Solvents for the 21st Century, ACS Sustain. Chem. Eng. 2 (2014) 1063–1071, https://doi.org/10.1021/sc500096j.

[13] Y. Liu, J.B. Friesen, J.B. McAlpine, D.C. Lankin, S.N. Chen, G.F. Pauli, Natural Deep Eutectic Solvents: Properties, Applications, and Perspectives, J. Nat. Prod. 81 (2018) 679–690, https://doi.org/10.1021/acs.jnatprod.7b00945.

[14] C. Florindo, L.C. Branco, I.M. Marrucho, Quest for Green-Solvent Design: From Hydrophilic to Hydrophobic (Deep) Eutectic Solvents, ChemSusChem 12 (2019) 1549–1559, https://doi.org/10.1002/cssc.201900147.

[15] T.R. Sekharan, R.M. Chandira, S. Tamilvanan, S.C. Rajesh, B.S. Venkateswarlu, Deep eutectic solvents as an alternate to other harmful solvents, Biointerface Res Appl Chem. 12 (2022) 847–860. https://doi.org/10.33263/BRIAC121.847860.

[16] E.L. Smith, A.P. Abbott, K.S. Ryder, Deep Eutectic Solvents (DESs) and Their Applications, Chem. Rev. 114 (2014) 11060–11082, https://doi.org/10.1021/cr300162p.

[17] B.B. Hansen, S. Spittle, B. Chen, D. Poe, Y. Zhang, J.M. Klein, A. Horton, L. Adhikari, T. Zelovich, B.W. Doherty, B. Gurkan, E.J. Maginn, A. Ragauskas, M. Dadmun, T.A. Zawodzinski, G.A. Baker, M.E. Tuckerman, R.F. Savinell, J. R. Sangoro, Deep Eutectic Solvents: A Review of Fundamentals and Applications, Chem. Rev. 121 (2021) 1232–1285, https://doi.org/10.1021/acs.chemrev.0c00385.

[18] M.F. Ahmer, Q. Ullah, Development and applications of deep eutectic solvents in different chromatographic techniques, JPC – Journal of Planar Chromatography – Modern TLC. 35 (2022) 549–570, https://doi.org/10.1007/s00764-022-00216-x.

[19] A.R. Jesus, L. Meneses, A.R.C. Duarte, A. Paiva, Natural deep eutectic systems—A new era of cryopreservation, in (2021:) 385–409, https://doi.org/10.1016/bs.abr.2020.09.015.

[20] M. Ivanović, M. Islamčević Razboršek, M. Kolar, Innovative Extraction Techniques Using Deep Eutectic Solvents and Analytical Methods for the Isolation and Characterization of Natural Bioactive Compounds from Plant Material, Plants. 9 (2020) 1428. https://doi.org/10.3390/plants9111428.

[21] S.C. Cunha, J.O. Fernandes, Extraction techniques with deep eutectic solvents, TrAC Trends Anal. Chem. 105 (2018) 225–239, https://doi.org/10.1016/j.trac.2018.05.001.

[22] M. Espino, M. de los Ángeles Fernández, F.J.V. Gomez, M.F. Silva, Natural designer solvents for greening analytical chemistry, TrAC Trends Anal. Chem. 76 (2016) 126–136, https://doi.org/10.1016/j.trac.2015.11.006.

[23] M. de los Á. Fernández, J. Boiteux, M. Espino, F.J.V. Gomez, M.F. Silva, Natural deep eutectic solvents-mediated extractions: The way forward for sustainable analytical developments, Anal Chim Acta. 1038 (2018) 1–10. https://doi.org/10.1016/j.aca.2018.07.059.

[24] C. Cannavacciuolo, S. Pagliari, J. Frigerio, C.M. Giustra, M. Labra, L. Campone, Natural Deep Eutectic Solvents (NADESs) Combined with Sustainable Extraction Techniques: A Review of the Green Chemistry Approach in Food Analysis, Foods. 12 (2022) 56, https://doi.org/10.3390/foods12010056.

[25] S. Kaoui, B. Chebli, S. Zaidouni, K. Basaid, Y. Mir, Deep eutectic solvents as sustainable extraction media for plants and food samples: A review, Sustain. Chem. Pharm. 31 (2023), 100937, https://doi.org/10.1016/j.scp.2022.100937.

[26] K. Wu, J. Ren, Q. Wang, M. Nuerjiang, X. Xia, C. Bian, Research Progress on the Preparation and Action Mechanism of Natural Deep Eutectic Solvents and Their Application in Food, Foods. 11 (2022) 3528, https://doi.org/10.3390/foods11213528.

[27] L. Lomba, C.B. García, M.P. Ribate, B. Giner, E. Zuriaga, Applications of Deep Eutectic Solvents Related to Health, Synthesis, and Extraction of Natural Based Chemicals, Appl. Sci. 11 (2021) 10156, https://doi.org/10.3390/app112110156.

[28] F. Mohd Fuad, M. Mohd Nadzir, A. Harun@Kamaruddin,, Hydrophilic natural deep eutectic solvent : A review on physicochemical properties and extractability of bioactive compounds, J. Mol. Liq. 339 (2021) 116923, https://doi.org/10.1016/j.molliq.2021.116923.

[29] J. Zuo, S. Geng, Y. Kong, P. Ma, Z. Fan, Y. Zhang, A. Dong, Current Progress in Natural Deep Eutectic Solvents for the Extraction of Active Components from Plants, Crit. Rev. Anal. Chem. 53 (2023) 177–198, https://doi.org/10.1080/10408347.2021.1946659.

[30] F.S.N. de Oliveira, A.R.C. Duarte, A look on target-specificity of eutectic systems based on natural bioactive compounds, in: 2021: pp. 271–307. https://doi.org/10.1016/bs.abr.2020.09.008.

[31] A. Mišan, M. Pojić, Applications of NADES in stabilizing food and protecting food compounds against oxidation, in: 2021: pp. 333–359. https://doi.org/10.1016/bs.abr.2020.09.010.

[32] D. Skarpalezos, A. Detsi, Deep Eutectic Solvents as Extraction Media for Valuable Flavonoids from Natural Sources, Appl. Sci. 9 (2019) 4169, https://doi.org/10.3390/app9194169.

[33] A. Mišan, J. Nađpal, A. Stupar, M. Pojić, A. Mandić, R. Verpoorte, Y.H. Choi, The perspectives of natural deep eutectic solvents in agri-food sector, Crit. Rev. Food Sci. Nutr. 60 (2020) 2564–2592, https://doi.org/10.1080/10408398.2019.1650717.

[34] A.V. Chemat, K. Ravi, P. Hilali, Tixier, Review of Alternative Solvents for Green Extraction of Food and Natural Products: Panorama, Principles, Applications and Prospects, Molecules 24 (2019) 3007, https://doi.org/10.3390/molecules24163007.

[35] L. Wils, S. Hilali, L. Boudesocque-Delaye, Biomass Valorization Using Natural Deep Eutectic Solvents: What's New in France? Molecules 26 (2021) 6556, https://doi.org/10.3390/molecules26216556.

[36] S. Mehariya, F. Fratini, R. Lavecchia, A. Zuorro, Green extraction of value-added compounds form microalgae: A short review on natural deep eutectic solvents (NaDES) and related pre-treatments, J. Environ. Chem. Eng. 9 (2021), 105989, https://doi.org/10.1016/j.jece.2021.105989.

[37] M. Jablonský, J. Šima, Phytomass Valorization by Deep Eutectic Solvents—Achievements, Perspectives, and Limitations, Crystals (Basel). 10 (2020) 800, https://doi.org/10.3390/cryst10090800.

[38] C. Aneklaphakij, P. Chamnanpuen, S. Bunsupa, V. Satitpatipan, Recent Green Technologies in Natural Stilbenoids Production and Extraction: The Next Chapter in the Cosmetic Industry, Cosmetics 9 (2022) 91, https://doi.org/10.3390/cosmetics9050091.

[39] N.P.E. Hikmawanti, D. Ramadon, I. Jantan, A. Mun'im, Natural Deep Eutectic Solvents (NADES): Phytochemical Extraction Performance Enhancer for Pharmaceutical and Nutraceutical Product Development, Plants. 10 (2021) 2091. https://doi.org/10.3390/plants10102091.

[40] C. Benoit, C. Virginie, V. Boris, The use of NADES to support innovation in the cosmetic industry, in: 2021: pp. 309–332. https://doi.org/10.1016/bs.abr.2020.09.009.

[41] M.S. Álvarez, Y. Zhang, Sketching neoteric solvents for boosting drugs bioavailability, J. Control. Release 311–312 (2019) 225–232, https://doi.org/10.1016/j.jconrel.2019.09.008.

[42] D.J.G.P. van Osch, L.F. Zubeir, A. van den Bruinhorst, M.A.A. Rocha, M.C. Kroon, Hydrophobic deep eutectic solvents as water-immiscible extractants, Green Chem. 17 (2015) 4518–4521, https://doi.org/10.1039/c5gc01451d.

[43] D.O. Abranches, M.A.R. Martins, L.P. Silva, N. Schaeffer, S.P. Pinho, J.A.P. Coutinho, Phenolic hydrogen bond donors in the formation of non-ionic deep eutectic solvents: The quest for type v des, Chem. Commun. 55 (2019) 10253–10256, https://doi.org/10.1039/c9cc04846d.

[44] D.O. Abranches, J.A.P. Coutinho, Type V deep eutectic solvents: Design and applications, Curr Opin Green Sustain Chem. 35 (2022), 100612, https://doi.org/10.1016/j.cogsc.2022.100612.

[45] N. Schaeffer, J.H.F. Conceica̅o̅, M.A.R. Martins, M.C. Neves, G. Pérez-Sánchez, J.R. B. Gomes, N. Papaiconomou, J.A.P. Coutinho, Non-ionic hydrophobic eutectics-versatile solvents for tailored metal separation and valorisation, Green Chem. 22 (2020) 2810–2820, https://doi.org/10.1039/d0gc00793e.

[46] I.M. Aroso, R. Craveiro, Â. Rocha, M. Dionísio, S. Barreiros, R.L. Reis, A. Paiva, A.R. C. Duarte, Design of controlled release systems for THEDES—Therapeutic deep eutectic solvents, using supercritical fluid technology, Int. J. Pharm. 492 (2015) 73–79, https://doi.org/10.1016/j.ijpharm.2015.06.038.

[47] O.G. Sas, L. Villar, Á. Domínguez, B. González, E.A. Macedo, Hydrophobic deep eutectic solvents as extraction agents of nitrophenolic pollutants from aqueous systems, Environ. Technol. Innov. 25 (2022), 102170, https://doi.org/10.1016/j.eti.2021.102170.

[48] D. Rodríguez-Llorente, A. Cañada-Barcala, S. Álvarez-Torrellas, V.I. Águeda, J. García, M. Larriba, A review of the use of eutectic solvents, terpenes and terpenoids in liquid–liquid extraction processes, Processes. 8 (2020) 1–54, https://doi.org/10.3390/pr8101220.

[49] G. Almustafa, R. Sulaiman, M. Kumar, I. Adeyemi, H.A. Arafat, I. AlNashef, Boron extraction from aqueous medium using novel hydrophobic deep eutectic solvents, Chem. Eng. J. 395 (2020), 125173, https://doi.org/10.1016/j.cej.2020.125173.

[50] X. Wei, Y. Wang, J. Chen, F. Xu, Z. Liu, X. He, H. Li, Y. Zhou, Adsorption of pharmaceuticals and personal care products by deep eutectic solvents-regulated magnetic metal-organic framework adsorbents: Performance and mechanism, Chem. Eng. J. 392 (2020), 124808, https://doi.org/10.1016/j.cej.2020.124808.

[51] D.J.G.P. Van Osch, C.H.J.T. Dietz, S.E.E. Warrag, M.C. Kroon, The Curious Case of Hydrophobic Deep Eutectic Solvents: A Story on the Discovery, Design, and Applications, ACS Sustain Chem Eng. 8 (2020) 10591–10612, https://doi.org/10.1021/acssuschemeng.0c00559.

[52] D. Lapeña, L. Lomba, M. Artal, C. Lafuente, B. Giner, Thermophysical characterization of the deep eutectic solvent choline chloride:ethylene glycol and one of its mixtures with water, Fluid Phase Equilib. 492 (2019) 1–9, https://doi.org/10.1016/j.fluid.2019.03.018.

[53] D. Lapeña, L. Lomba, M. Artal, C. Lafuente, B. Giner, The NADES glyceline as a potential Green Solvent: A comprehensive study of its thermophysical properties and effect of water inclusion, J. Chem. Thermodyn. 128 (2019) 164–172, https://doi.org/10.1016/j.jct.2018.07.031.

[54] D. Lapeña, F. Bergua, L. Lomba, B. Giner, C. Lafuente, A comprehensive study of the thermophysical properties of reline and hydrated reline, J. Mol. Liq. 303 (2020), 112679, https://doi.org/10.1016/j.molliq.2020.112679.

[55] F. Bergua, M. Castro, C. Lafuente, M. Artal, Thymol+l-menthol eutectic mixtures: Thermophysical properties and possible applications as decontaminants, J. Mol. Liq. 368 (2022), 120789, https://doi.org/10.1016/j.molliq.2022.120789.

[56] F. Bergua, M. Castro, J. Muñoz-Embid, C. Lafuente, M. Artal, L-menthol-based eutectic solvents: Characterization and application in the removal of drugs from water, J. Mol. Liq. 352 (2022), 118754, https://doi.org/10.1016/j.molliq.2022.118754.

[57] F. Bergua, M. Castro, J. Muñoz-Embid, C. Lafuente, M. Artal, Hydrophobic eutectic solvents: Thermophysical study and application in removal of pharmaceutical products from water, Chem. Eng. J. 411 (2021), https://doi.org/10.1016/j.cej.2021.128472.

[58] P. Harten, T. Martin, M. Gonzalez, D. Young, The software tool to find greener solvent replacements, PARIS III, Environ Prog Sustain Energy. 39 (2020) 1–7, https://doi.org/10.1002/ep.13331.

[59] Y.A. Sanmamed, D. González-Salgado, J. Troncoso, C.A. Cerdeiriña, L. Romaní, Viscosity-induced errors in the density determination of room temperature ionic liquids using vibrating tube densitometry, Fluid Phase Equilib. 252 (2007) 96–102, https://doi.org/10.1016/j.fluid.2006.12.016.

[60] Z. Wagner, M. Bendová, J. Rotrekl, A. Sýkorová, M. Čanji, N. Parmar, Density and sound velocity measurement by an Anton Paar DSA 5000 density meter: Precision and long-time stability, J. Mol. Liq. 329 (2021), 115547, https://doi.org/10.1016/j.molliq.2021.115547.

[61] R.B. Leron, D.S.H. Wong, M.H. Li, Densities of a deep eutectic solvent based on choline chloride and glycerol and its aqueous mixtures at elevated pressures, Fluid Phase Equilib. 335 (2012) 32–38, https://doi.org/10.1016/j.fluid.2012.08.016.

[62] R.B. Leron, M.H. Li, High-pressure volumetric properties of choline chloride-ethylene glycol based deep eutectic solvent and its mixtures with water, Thermochim Acta 546 (2012) 54–60, https://doi.org/10.1016/j.tca.2012.07.024.

[63] E.A. Crespo, J.M.L. Costa, A.M. Palma, B. Soares, M.C. Martín, J.J. Segovia, P. J. Carvalho, J.A.P. Coutinho, Thermodynamic characterization of deep eutectic solvents at high pressures, Fluid Phase Equilib. 500 (2019), 112249, https://doi.org/10.1016/j.fluid.2019.112249.

[64] A. Mero, S. Koutsoumpos, P. Giannios, I. Stavrakas, K. Moutzouris, A. Mezzetta, L. Guazzelli, Comparison of physicochemical and thermal properties of choline chloride and betaine-based deep eutectic solvents: The influence of hydrogen bond acceptor and hydrogen bond donor nature and their molar ratios, J. Mol. Liq. 377 (2023), 121563, https://doi.org/10.1016/j.molliq.2023.121563.

[65] M.M. Abdallah, S. Müller, A.G. de Castilla, P. Gurikov, A.A. Matias, M.do R. Bronze, N. Fernández, Physicochemical Characterization and Simulation of the Eutectic Solvent Systems, Molecules 26 (2021) 1801–1816.

[66] P. Makoś, A. Przyjazny, G. Boczkaj, Hydrophobic deep eutectic solvents as "green" extraction media for polycyclic aromatic hydrocarbons in aqueous samples, J. Chromatogr. A 1570 (2018) 28–37, https://doi.org/10.1016/j.chroma.2018.07.070.

[67] K. Li, Y. Jin, D. Jung, K. Park, H. Kim, J. Lee, In situ formation of thymol-based hydrophobic deep eutectic solvents: Application to antibiotics analysis in surface water based on liquid-liquid microextraction followed by liquid chromatography, J. Chromatogr. A 1614 (2020), https://doi.org/10.1016/j.chroma.2019.460730.

[68] A. Kovács, E.C. Neyts, I. Cornet, M. Wijnants, P. Billen, Modeling the Physicochemical Properties of Natural Deep Eutectic Solvents, ChemSusChem 13 (2020) 3789–3804, https://doi.org/10.1002/cssc.202000286.

[69] S. Stephan, J. Staubach, H. Hasse, Review and comparison of equations of state for the Lennard-Jones fluid, Fluid Phase Equilib. 523 (2020), 112772, https://doi.org/10.1016/j.fluid.2020.112772.

[70] G.M. Kontogeorgis, A. Schlaikjer, M.D. Olsen, B. Maribo-Mogensen, K. Thomsen, N. von Solms, X. Liang, A Review of Electrolyte Equations of State with Emphasis on Those Based on Cubic and Cubic-Plus-Association (CPA) Models, Int. J. Thermophys. 43 (2022) 54, https://doi.org/10.1007/s10765-022-02976-4.

[71] L. Fernandez, L.P. Silva, M.A.R. Martins, O. Ferreira, J. Ortega, S.P. Pinho, J.A. P. Coutinho, Indirect assessment of the fusion properties of choline chloride from solid-liquid equilibria data, Fluid Phase Equilib. 448 (2017) 9–14, https://doi.org/10.1016/j.fluid.2017.03.015.

[72] W.G. Linstrom, P.J.; Mallard, NIST Chemistry Webbok, NIST Standard Reference Database Number 69, Gaithersburg MD, 20899, 2020. https://doi.org/10.18434/T4D303.

[73] H. Guerrero, M. García-Mardones, P. Cea, C. Lafuente, I. Bandrés, Correlation of the volumetric behaviour of pyridinium-based ionic liquids with two different equations, Thermochim Acta 531 (2012) 21–27, https://doi.org/10.1016/j.tca.2011.12.020.

[74] J. Gross, G. Sadowski, Perturbed-chain SAFT: An equation of state based on a perturbation theory for chain molecules, Ind. Eng. Chem. Res. 40 (2001) 1244–1260, https://doi.org/10.1021/ie0003887.

[75] J. Gross, G. Sadowski, Application of perturbation theory to a hard-chain reference fluid: An equation of state for square-well chains, Fluid Phase Equilib. 168 (2000) 183–199, https://doi.org/10.1016/S0378-3812(00)00302-2.

[76] W.G. Chapman, G. Jackson, K.E. Gubbins, Phase equilibria of associating fluids, Mol. Phys. 65 (1988) 1057–1079, https://doi.org/10.1080/00268978800101601.

[77] J.A. Barker, D. Henderson, Perturbation Theory and Equation of State for Fluids: The Square-Well Potential, J. Chem. Phys. 47 (1967) 2856–2861, https://doi.org/10.1063/1.1712308.

[78] J.A. Barker, D. Henderson, Perturbation Theory and Equation of State for Fluids. II. A Successful Theory of Liquids, J. Chem. Phys. 47 (1967) 4714–4721, https://doi.org/10.1063/1.1701689.

[79] M.A.R. Martins, E.A. Crespo, P.V.A. Pontes, L.P. Silva, M. Bülow, G.J. Maximo, E.A. C. Batista, C. Held, S.P. Pinho, J.A.P. Coutinho, Tunable Hydrophobic Eutectic Solvents Based on Terpenes and Monocarboxylic Acids, ACS Sustain. Chem. Eng. 6 (2018) 8836–8846, https://doi.org/10.1021/acssuschemeng.8b01203.

[80] L.F. Zubeir, C. Held, G. Sadowski, M.C. Kroon, PC-SAFT Modeling of CO2 Solubilities in Deep Eutectic Solvents, J. Phys. Chem. B 120 (2016) 2300–2310, https://doi.org/10.1021/acs.jpcb.5b07888.

[81] M. Atilhan, S. Aparicio, PρT measurements and derived properties of liquid 1,2-alkanediols, J. Chem. Thermodyn. 57 (2013) 137–144, https://doi.org/10.1016/j.jct.2012.08.014.

[82] C. Held, G. Sadowski, Compatible solutes: Thermodynamic properties relevant for effective protection against osmotic stress, Fluid Phase Equilib. 407 (2016) 224–235, https://doi.org/10.1016/j.fluid.2015.07.004.

[83] J. Troncoso, C.A. Cerdeiriña, P. Navia, Y.A. Sanmamed, D. González-Salgado, L. Romaní, Unusual Behavior of the Thermodynamic Response Functions of Ionic Liquids, J. Phys. Chem. Lett. 1 (2010) 211–214, https://doi.org/10.1021/jz900049g.

[84] E. Wilhelm, Pressure dependence of the isothermal compressibility and a modified form of the Tait equation, J. Chem. Phys. 63 (1975) 3379–3381, https://doi.org/10.1063/1.431774.

[85] V.N. Kartsev, S.N. Shtykov, K.E. Pankin, D.V. Batov, Intermolecular forces and the internal pressure of liquids, J. Struct. Chem. 53 (2012) 1087–1093, https://doi.org/10.1134/S0022476612060108.

[86] J.H. Hildebrand, Solubility of non-electrolytes. By J. H. Hildebrand, Ph.D. 2nd ed. Pp. 203. New York: Reinhold Publishing Corp., London: Chapman & Hall, Ltd., 1936. 22s. 6d, Journal of the Society of Chemical Industry. 55 (1936) 665–665. https://doi.org/10.1002/jctb.5000553408.

[87] J.M.S.E.B. Bagley, T.P. Nelson, Three-dimensional solubility parameters and their relationship to internal pressure measurements in polar and hydrogen bonding solvents, J Paint Technol. 43 (1971) 35–42.